

Combined NMR, SAXS, and DLS Study of Concentrated Clear Solutions Used in Silicalite-1 Zeolite Synthesis

Alexander Aerts,[†] Lana R. A. Follens,[†] Mohamed Haouas,[‡] Tom P. Caremans,[†]
 Marc-André Delsuc,[§] Benoit Loppinet,^{||} Jan Vermant,[⊥] Bart Goderis,[#] Francis Taulelle,[‡]
 Johan A. Martens,[†] and Christine E. A. Kirschhock^{*,†}

Centre for Surface Chemistry and Catalysis, K.U. Leuven, Kasteelpark Arenberg 23, B-3001 Heverlee, Belgium, Institut Lavoisier, Université de Versailles St. Quentin en Yvelines, 45 avenue des Etats-Unis, F-78035 Versailles, France, Centre de Biochimie Structurale, 29 rue de Navacelles, F-34090 Montpellier, France, IESL-FORTH, P.O. Box 1527, GR-711 10 Heraklion, Greece, Department of Chemical Engineering, K.U. Leuven, Willem de Croylaan 46, B-3001 Heverlee, Belgium, and Department of Chemistry, K.U. Leuven, Celestijnenlaan 200f, B-3001 Heverlee, Belgium

Received March 13, 2007. Revised Manuscript Received May 8, 2007

Concentrated clear solutions, as used for the preparation of Silicalite-1 zeolite, were synthesized from tetrapropylammonium hydroxide, tetraethylorthosilicate, and water. The solutions were analyzed using three techniques: quantitative ²⁹Si NMR, synchrotron small-angle X-ray scattering (SAXS), and dynamic light scattering (DLS). ²⁹Si NMR showed the coexistence of silicate oligomers and particles. For the first time, both fractions were analyzed simultaneously, providing a global, quantitative description of the clear solution microstructure. The SAXS patterns, typical of interacting particles, could be used together with the ²⁹Si NMR deduced particle volume fraction to estimate a particle size. A careful analysis of DLS data of the dynamics of the suspensions revealed the occurrence of two diffusive processes. The faster process is a collective particle diffusion. The slower process corresponds to the particle self-diffusion and is present because of the presence of polydispersity in size, shape, and/or surface charge. The self-diffusion coefficient provides a means to estimate the equivalent hydrodynamic radius. The observations hence reveal a complex, polydisperse mixture of particles present at the onset of the Silicalite-1 zeolite formation. Implications on the proposed zeolite formation mechanisms are briefly discussed.

Introduction

Initiated by the pioneering work of Schoeman et al.,¹ the so-called clear solution synthesis of Silicalite-1 has become the model system for the study of zeolite formation. In a clear solution, particles smaller than 5 nm are formed at room temperature. Despite the fact that these particles have been extensively investigated, much controversy remains regarding their structure, shape, and role in the formation of zeolite crystals upon hydrothermal treatment. The nanoparticle structure has been interpreted as being anything between amorphous² and fully structured.³ Correspondingly, the assigned role of the particles in the crystallization varies from a mere monomer reservoir⁴ to the MFI building block.⁵ At the origin of these diverging interpretations lies the difficulty

in interpreting various experimental observations on clear solutions, especially at high concentrations. More specifically, in scattering experiments, like small-angle X-ray and neutron scattering (SAXS and SANS) and dynamic light scattering (DLS), particle interactions strongly affect the measurement and make the interpretation more difficult. The problem of particle interaction can usually be circumvented by strongly diluting the suspensions^{2a} and/or screening electrostatic interactions, but in this specific case it remains an open question whether the data obtained on diluted systems are representative for concentrated suspensions. In the present work SAXS data on concentrated clear solutions are analyzed using a quantification of the particle populations obtained by ²⁹Si NMR.

Experimental Section

To prepare the clear solutions, an amount of tetraethylorthosilicate (TEOS) (Acros, 98%) was hydrolyzed in aqueous tetrapropyl-

* To whom correspondence should be addressed: E-mail: christine.kirschhock@biw.kuleuven.be.

[†] Centre for Surface Chemistry and Catalysis, K.U. Leuven.

[‡] Université de Versailles St. Quentin en Yvelines.

[§] Centre de Biochimie Structurale.

^{||} IESL-FORTH.

[⊥] Department of Chemical Engineering, K.U. Leuven.

[#] Department of Chemistry, K.U. Leuven.

- (1) (a) Schoeman, B. J.; Sterte, J.; Otterstedt, J. E. *Zeolites* **1994**, *14*, 568. (b) Persson, A. E.; Schoeman, B. J.; Sterte, J.; Otterstedt, J. E. *Zeolites* **1994**, *14*, 557. (c) Schoeman, B. J.; Regev, O. *Zeolites* **1996**, *17*, 447. (d) Schoeman, B. J. *Microporous Mater.* **1997**, *9*, 267.
- (2) (a) Fedeyko, J. M.; Vlachos, D. G.; Lobo, R. F. *Langmuir* **2005**, *21*, 5197. (b) Rimer, J. D.; Fedeyko, J. M.; Vlachos, D. G.; Lobo, R. F. *Chem.-Eur. J.* **2006**, *12*, 2926. (c) Ramanan, H.; Kokkoli, E.; Tsapatsis, M. *Angew. Chem.* **2004**, *116*, 4658; *Angew. Chem., Int. Ed.* **2004**, *43*, 4558.

- (3) (a) Ravishankar, R.; Kirschhock, C. E. A.; Knops-Gerrits, P. P.; Feijen, E. J. P.; Grobet, P. J.; Vanoppen, P.; De Schryver, F. C.; Mieke, G.; Fuess, H.; Schoeman, B. J.; Jacobs, P. A.; Martens, J. A. *J. Phys. Chem. B* **1999**, *103*, 4960. (b) Kirschhock, C. E. A.; Buschmann, V.; Kremer, S.; Ravishankar, R.; Houssin, C. J. Y.; Mojet, B. L.; van Santen, R. A.; Grobet, P. J.; Jacobs, P. A.; Martens, J. A. *Angew. Chem.* **2001**, *113*, 2707; *Angew. Chem., Int. Ed.* **2001**, *40*, 2637.
- (4) Cundy, C. S.; Cox, P. A. *Microporous Mesoporous Mater.* **2005**, *82*, 1.
- (5) Kirschhock, C. E. A.; Ravishankar, R.; Jacobs, P. A.; Martens, J. A. *J. Phys. Chem. B* **1999**, *103*, 11021.

Table 1. Composition, pH, and Viscosity (η) of the Studied Clear Solutions

x^a	f_{Si}^b (10^{-3} mol/g solution)	pH	η (mPa·s)
5	1.86	11.7	6.8
9	1.76	12.5	6.7
13	1.66	13.0	10.2
19	1.54	13.6	12.9

^a Molar TPAOH content of the clear solutions with composition TEOS/TPAOH/H₂O 25: x :400. ^b Molar Si content of the clear solutions.

ammonium hydroxide (TPAOH) solution (Alfa, 40 wt %) at room temperature under magnetic stirring. Hydrolysis occurred in approximately 10 min. After 15 additional minutes, water was added to obtain the desired molar TEOS/TPAOH/H₂O ratios of 25: x :400, where x = 5, 9, 13, and 19. The samples were prepared in 20 mL quantities. As pH and viscosity change with TPAOH content both parameters were monitored. The suspension viscosity was measured using a rolling ball viscosimeter from Anton Paar at 25.0 °C; 24 h after sample preparation the pH was measured at room temperature using a WTW pH 353 equipped with a glass electrode. The electrode was immersed in each sample, and a stable read-out was obtained after ± 15 min. Between successive measurements the electrode was cleaned with water. The pH and viscosity of the clear solutions are given in Table 1.

The ²⁹Si NMR experiments were carried out with 10 mm fused silica tubes, in a modified background free probe, using a Bruker Avance 500 spectrometer operating at a resonance frequency of 99.353 MHz. The spectra were recorded with single-pulse acquisition at room temperature (24–25 °C) using a pulse of 8.5 μ s (45°), a repeating time of 7 s, and 8192 accumulations.

Two-dimensional (2D) SAXS patterns of solutions loaded in glass capillaries (Hilgenberg, 1 mm diameter) were recorded at the European Synchrotron Radiation Facility (ESRF, Grenoble, France) on Beamline BM-26B (DUBBLE). The scattering patterns were recorded with a gas-filled detector, at a distance of 1.50 m from the sample. The accumulation time per SAXS pattern was 60 s. The intensity I as a function of scattering vector (q) was obtained by radially averaging the 2D patterns, after applying the corrections for transmission and empty cell background. The q -axis was calibrated using Ag Behenate crystals.

DLS measurements were performed at 25.0 °C on an ALV CGS-3 apparatus, recording the autocorrelation functions (ACFs) as $g_2(t) - 1$. Two milliliters of each sample was loaded in borosilicate glass tubes with a height of 7.5 cm and an external diameter of 8 mm. The sample tubes were inserted in the sample compartment of the apparatus, using toluene (n = 1.49) as index matching fluid. The time-averaged intensity and the intensity autocorrelation was measured at 6–10 scattering angles between 25 and 150° for 60 s for samples x = 5 and 9. A longer accumulation time of 600 s (20 runs of 30 s) was adopted for samples x = 13 and 19.

Results

²⁹Si NMR. Quantitative ²⁹Si NMR spectra of the four clear solutions with different TPAOH contents (Figure 1) revealed sharp lines (line width \sim 1 Hz) superimposed on broad bands (line width \sim 100–700 Hz). The sharp signals are caused by dissolved silicate oligomers; the broad bands, caused by slowly moving silicon, can be identified as originating from the particles. The assignment of broad bands to particles is validated by the spectra of the samples x = 5 and 9, which are known to contain nanometer-size particles according to

previously⁶ reported SAXS measurements, which were confirmed in the present work (vide infra). The applied liquid-state NMR conditions allow a quantitative observation of all Si contained in the samples. The ²⁹Si NMR spectra can hence be decomposed to quantify the relative amount of particle and oligomer fraction (Figure 2a). Low TPAOH content x favors the formation of particles over oligomers. Interestingly, the ²⁹Si NMR spectra of the samples with x = 5 and 9 also show broadened signals in the Q^4 chemical shift region around -110 ppm (Figure 1a,b), confirming the increased degree of condensation of these particles. The systematic variation of the broadened components of the recorded spectra with sample composition and careful exclusion of experimental artifacts shows that the Q environments observed are intrinsic to the sample and not caused by background signals of the NMR probe head or the sample tube, as suggested in literature in an investigation of a similar clear solution.⁷

Combined SAXS and SANS investigations on dilute clear solutions revealed a core-shell structure of particles with a TPA-rich shell and a silica-rich core. However, in SAXS experiments the low contrast difference between shell and solvent cannot be resolved, so SAXS mainly accesses the silica-rich core.^{2a} The present quantitative NMR analysis can be used to estimate a particle volume fraction ϕ that pertains, like the SAXS analysis, to the silica only. This particle volume fraction ϕ was obtained from the fraction of silicon atoms present in particles (f_p) determined with quantitative ²⁹Si NMR (Figure 1a) using

$$\phi = \frac{NV_p}{V_s} = \frac{f_{\text{Si}}\rho_s f_p W_p}{\rho_p} \quad (1)$$

where N is the number of particles, V_p is the particle volume, V_s is the solution volume, f_{Si} is the molar Si content (mol/g solution), ρ_s is the solution density (~ 1 g/cm³), and ρ_p is the silica density. The latter was taken to be 1.75 g/cm³ as determined on material isolated from comparable solutions.^{2a} In eq 1, W_p refers to the formula weight of the particles which takes the polymerization degree into account. For a fully condensed silica particle, the bulk chemical formula corresponds to SiO₂ and the formula weight is 60.1 g/mol. Less internally condensed particles are represented by the SiO_y formula with y larger than 2. In this formula, hydrogen atoms of hydroxyl groups are neglected for convenience. The stoichiometric coefficient y , required to calculate the formula weight W_p of the particles of the four samples (Table 2), was derived from the Q^n distribution of the particles (Figure 2b) according to

$$y = \frac{\text{O}}{\text{Si}} = \sum_{n=0}^4 Q^n \left(4 - \frac{1}{n} \right) \quad (2)$$

The particle volume fraction ϕ of the four investigated clear solutions is found to decrease from 0.070 at x = 5 to 0.030 at x = 19 as listed in Table 2.

(6) Cheng, C. H.; Shantz, D. F. *Curr. Opin. Colloid Interface Sci.* **2005**, *10*, 188.

(7) Cheng, C. H.; Shantz, D. F. *J. Phys. Chem. B* **2006**, *110*, 313.

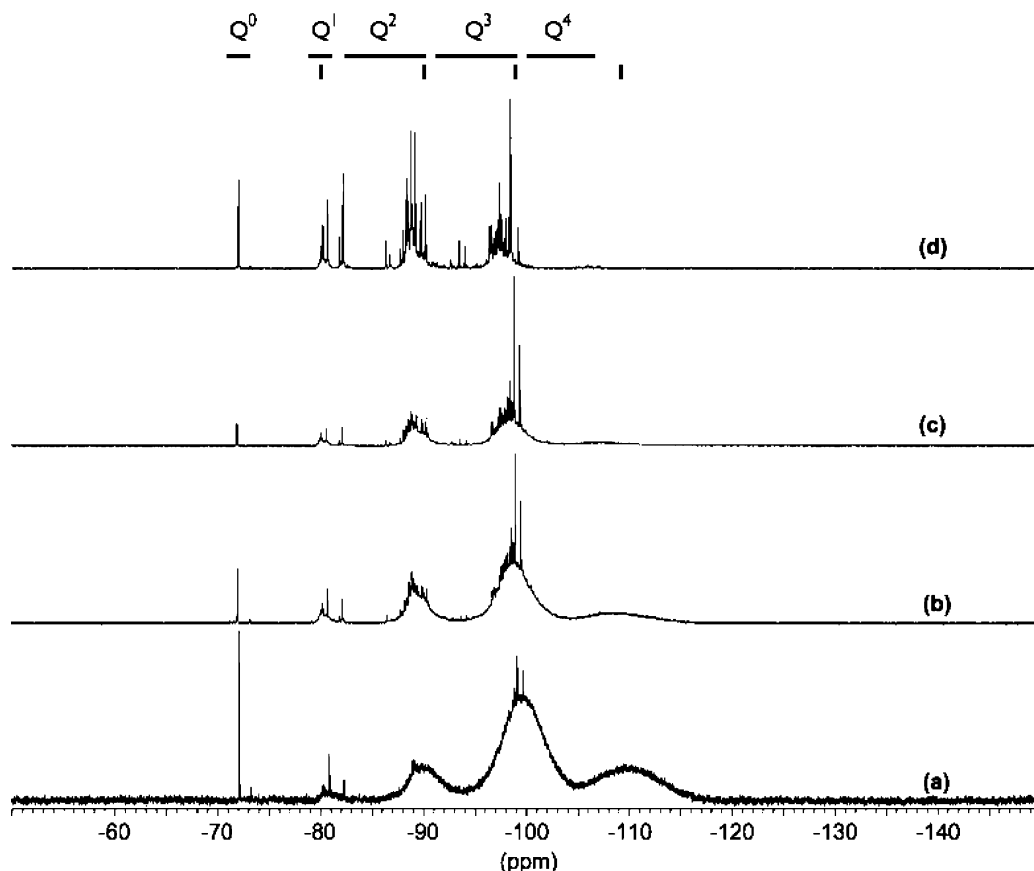


Figure 1. Quantitative ^{29}Si NMR spectra of clear solutions with TEOS:TPAOH:H₂O molar ratio of 25: x :400 where (a) $x = 5$, (b) $x = 9$, (c) $x = 13$, and (d) $x = 19$. The oligomer Q^n ranges are indicated. The markers indicate the position of the particle broad bands.

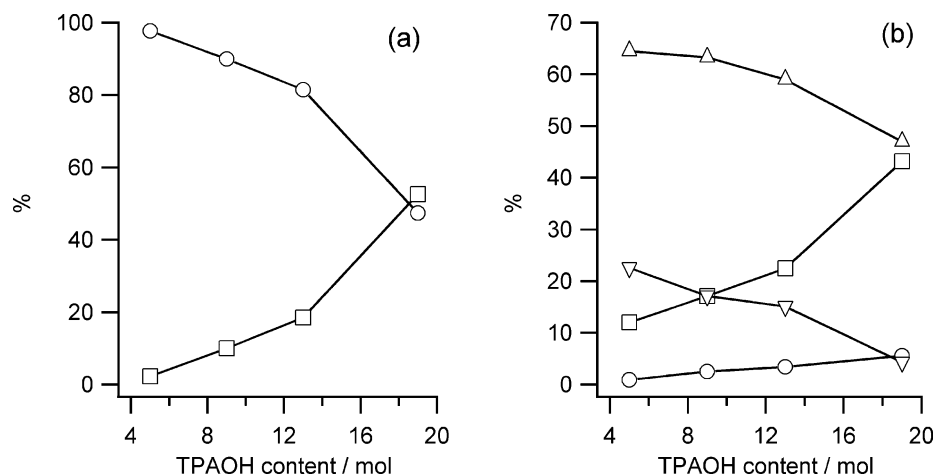


Figure 2. (a) Fraction of silicon present as particles (circles) and oligomers (squares); (b) silicon Q^n distribution of the particle fraction: Q^1 , circles; Q^2 , squares; Q^3 , up triangles; and Q^4 , down triangles.

SAXS. The scattered intensities as a function of scattering vector for the four clear solutions are presented in Figure 3. All patterns exhibited a well marked broad intensity maximum. The q value associated with the intensity maximum, q_{max} , increased with increasing x (Table 2), confirming earlier observations.⁸ The occurrence of an intensity maximum is attributed to the correlation of the particle positions due to interparticle interactions. In addition to a form factor, which describes the particle properties, the structure factor con-

tributes to the scattered intensity, accounting for the interparticle interactions. A frequently used technique to determine the structure factor is to dilute the system sufficiently to reduce particle interactions. While this technique is appropriate with inert particles, in clear solutions with reactive silicate, the particles may be changed upon dilution. In view of the strong sensitivity of the particle content of clear solutions with changing composition (Figure 2a), such a particle change upon dilution is highly probable and a renormalization by the dilute suspensions' form factor is not possible.

(8) Yang, S.; Navrotsky, A.; Wesolowski, D. J.; Pople, J. A. *Chem. Mater.* **2004**, *16*, 210.

Table 2. Suspension and Particle Characteristics as a Function of the TPAOH Content x

x^a	y^b	f_p^c	W_p^d (g/mol)	ϕ^e (10^{-3})	q_{\max}^f (nm^{-1})	d_{SAXS}^g (nm)	$d_{\text{DLS,slow}}^h$ (nm)
5	2.46	0.977	67.4	70	1.28	2.9	4.5
9	2.53	0.900	68.5	62	1.47	2.4	2.4
13	2.57	0.815	69.1	53	2.80	1.2	1.5
19	2.75	0.474	72.0	30	3.39	0.8	1.0

^a Molar TPAOH content of the studied clear solutions with composition TEOS/TPAOH/H₂O 25: x :400. ^b Stoichiometric coefficient y in SiO _{y} formula. ^c Fraction of total silicon atoms inside particles. ^d Formula weight of the particles in g/mol. ^e Particle volume fraction. ^f q value associated with the intensity maximum in the SAXS pattern. ^g Particle diameter in nm calculated from q_{\max} using eq 3. ^h Particle diameter in nm calculated from the diffusion coefficient associated with the slow mode using the Stokes–Einstein equation.

Nonetheless, as the quantitative ²⁹Si NMR provides the silica volume fraction independently (Table 2), a simplified approach to separate structure factor and form effects can be adopted. The peak position q_{\max} can now be used to extract an estimate particle size. Assuming repulsive, spherical particles, the peak position D^* expressed in length scale is given by an approximate empirical expression:⁹

$$D^* = \frac{2\pi}{q_{\max}} = \frac{1}{\sqrt{2}} \left(\frac{8\pi}{3} \right)^{1/3} \frac{d_{\text{SAXS}}}{2\phi^{1/3}} \quad (3)$$

The result of the particle size estimation by the combined SAXS–NMR analysis is given in Table 2. The equivalent spherical particle diameter d_{SAXS} is estimated at 2.9 nm for a TPAOH content x of 5. At the highest TPAOH content of $x = 19$, an estimate of 0.8 nm is obtained (Table 2). At $x = 19$, the Q^n connectivity of the particles, $Q^1/Q^2/Q^3/Q^4$ of 5.6:43.2:47.0:4.3 is very similar to that of the oligomers having a $Q^1/Q^2/Q^3/Q^4$ distribution of 5.9:46.1:47.1:1.0. Hence, for this particular sample, the small particles likely are physically associated oligomers. The Q^n distribution of the particles at $x = 9$ ($Q^2/Q^3/Q^4$ of 17.1:63.3:17.1) approaches that of the previously described Si₃₃ precursor ($Q^2/Q^3/Q^4$ of 12:73:15), characterized after extraction of the silicate species from a similar clear solution.^{3a,10} On the basis of earlier studies of solids extracted from a clear solution with $x = 9$ the larger nanoslab model was proposed.^{3a,10} In clear solution, the present ²⁹Si NMR study shows that the silicate connectivity is less developed than in a nanoslab and, hence, better described by the smaller precursor unit.

DLS. Next to SAXS, DLS is another technique that has been used frequently to characterize the subcolloidal particles in Silicalite-1 syntheses.^{1,11} For dilute suspensions, in the absence of particle and hydrodynamic interactions, the intensity ACF decays exponentially. The ACF represents the relaxation of particle concentration fluctuations, with a wavelength in the order of $2\pi/q$, where q is the scattering

wave vector. In dilute suspensions, concentration fluctuations relax solely by Brownian motion of the nanoparticles, characterized by a self-diffusion coefficient D_0 . It is common practice to calculate the particle hydrodynamic diameter from D_0 using the Stokes–Einstein equation. This approach is, however, only valid for systems of non-interacting particles. For concentrated suspensions of interacting particles, as dealt with in the present study, a more elaborate analysis is required.

The ACFs obtained at different angles using DLS were analyzed using an inverse Laplace transform algorithm, regularized by entropy maximization (ILT-MEM), following Delsuc and Malliavin.¹² Some representative relaxation rate distribution functions are shown in Figure 4. Two distinct relaxation modes were observed in all samples studied. The two peaks in the relaxation rate distribution functions $G(\Gamma)$ could be described with Gauss curves. The average relaxation rate Γ of each mode and its associated amplitude were determined. The respective diffusion coefficients were obtained by plotting the relaxation rates Γ versus the square of the scattering vector q^2 (Figure 5). A linear relation between Γ and q^2 is found, indicating that both processes are diffusive. The diffusion coefficient D can be obtained from

$$\Gamma = \frac{1}{\tau} = Dq^2 \quad (4)$$

The DLS measurements yield two diffusion constants, D_f and D_s , the subscripts f and s referring to fast and slow mode, respectively. The D_f and D_s values are plotted against the molar TPAOH content x in Figure 6. Fast and slow diffusivities typically differed by about an order of magnitude.

The particle size obtained from the combined SAXS–NMR measurements (d_{SAXS} , Table 2), together with the viscosity η (Table 1), yielded an estimate of the expected self-diffusion coefficient D_0 by application of the Stokes–Einstein equation:

$$D_0 = \frac{kT}{6\pi\eta R} \quad (5)$$

with k being the Boltzmann constant, T being the temperature in kelvin, and R being the particle radius.

In Figure 6, D_0 was compared to the experimentally obtained diffusion coefficients D_f and D_s from DLS. D_s was found to be of the same order of magnitude as D_0 . This shows that equivalent hydrodynamic particle sizes can be determined reliably by measurement of D_s , provided the ACFs are adequately analyzed. The resulting hydrodynamic particle diameters derived from DLS, $d_{\text{DLS,slow}}$ are listed in Table 2. The $d_{\text{DLS,slow}}$ value is 4.5 nm for the lowest TPAOH content and decreases to 1.0 nm at the highest TPAOH content.

Discussion

As expected, the composition of the clear solutions has a strong effect on the average size and interaction strength of

- (9) Lindner, P.; Zemb, Th. *Neutrons, X-rays and Light: Scattering Methods Applied to Soft Condensed Matter*; Elsevier Science B.V.: Amsterdam, The Netherlands, 2002.
- (10) (a) Kirschhock, C. E. A.; Ravishankar, R.; Verspeurt, F.; Grobet, P. J.; Jacobs, P. A.; Martens, J. A. *J. Phys. Chem. B* **1999**, *103*, 4965. (b) Kirschhock, C. E. A.; Ravishankar, R.; Truyens, K.; Verspeurt, F.; Jacobs, P. A.; Martens, J. A. *Stud. Surf. Sci. Catal.* **2000**, *129*, 139.
- (11) Mintova, S.; Olson, N. H.; Senker, J.; Bein, T. *Angew. Chem.* **2002**, *114*, 2670; *Angew. Chem., Int. Ed.* **2002**, *14*, 2558.

- (12) Delsuc, M.; Malliavin, T. *Anal. Chem.* **1998**, *70*, 2146.

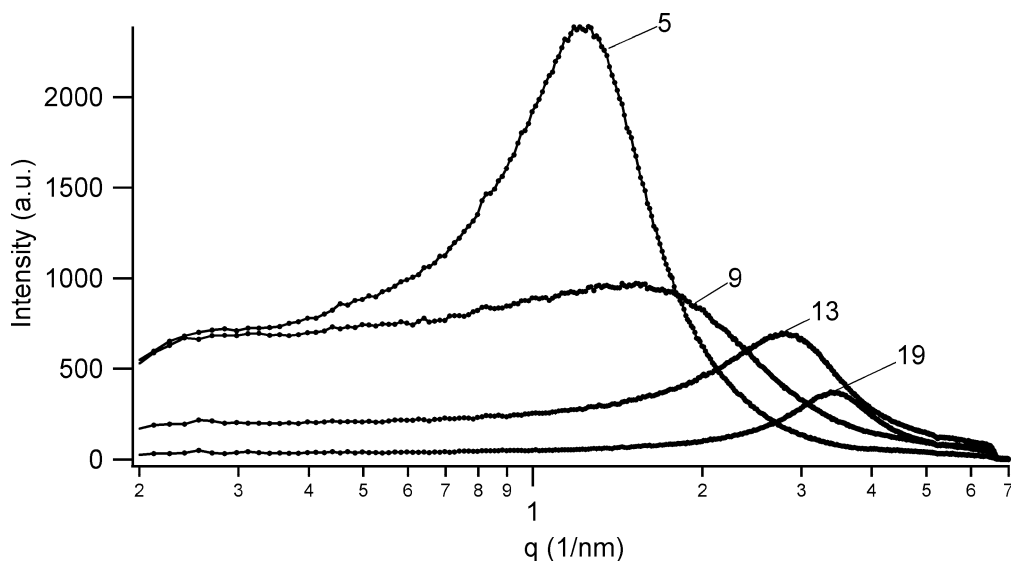


Figure 3. Scattered X-ray intensity as a function of scattering vector of clear solutions with a TEOS/TPAOH/H₂O molar ratio of 25:*x*:400 where *x* = 5, 9, 13, and 19.

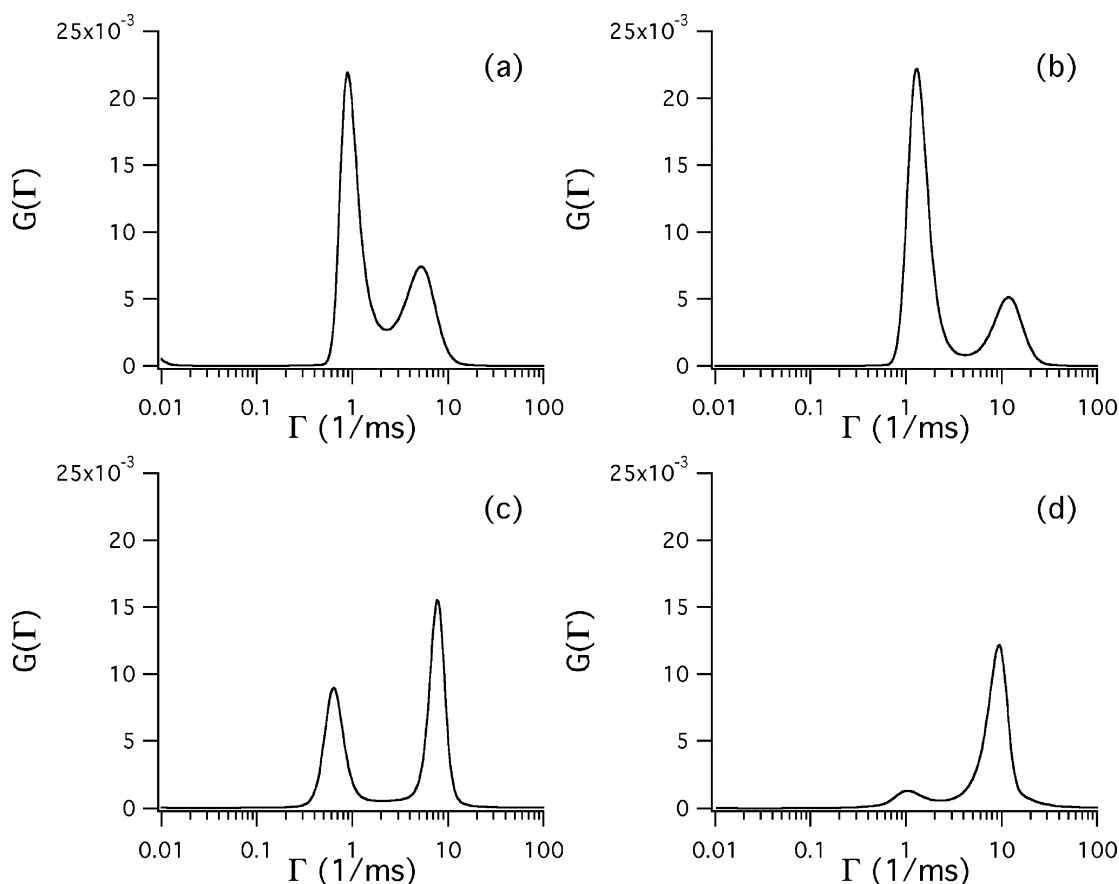


Figure 4. Relaxation rate distribution functions $G(\Gamma)$ of clear solutions with molar TPAOH content *x*. (a) *x* = 5 measured at a scattering angle of 30°, (b) *x* = 9 at 30°, (c) *x* = 13 at 35°, and (d) *x* = 19 at 35°.

the initially formed nanoparticles. This certainly is due to the rise of pH with increasing TPAOH concentration, but other parameters like viscosity and template–silicate interaction also play important roles. The combination of SAXS analysis with volume fractions derived by ²⁹Si NMR clearly demonstrates that the particle interaction in concentrated clear solutions manifests in a prominent structure factor. This has an important consequence for the recorded DLS spectra.

In previous DLS studies of concentrated Silicalite-1 clear solutions, the presence of a fast diffusive process has been overlooked.^{1d,11} In concentrated colloidal dispersions such as micro-emulsions and hard sphere dispersions, a similar two-mode behavior has been observed¹³ and attributed to collective and self-diffusion modes.^{13a,14} Collective diffusion

- (13) (a) Appell, J.; Porte, G.; Buhler, E. *J. Phys. Chem. B* **2005**, *109*, 13186.
(b) Yan, Y. D.; Clarke, J. H. R. *J. Chem. Phys.* **1990**, *93*, 4501.

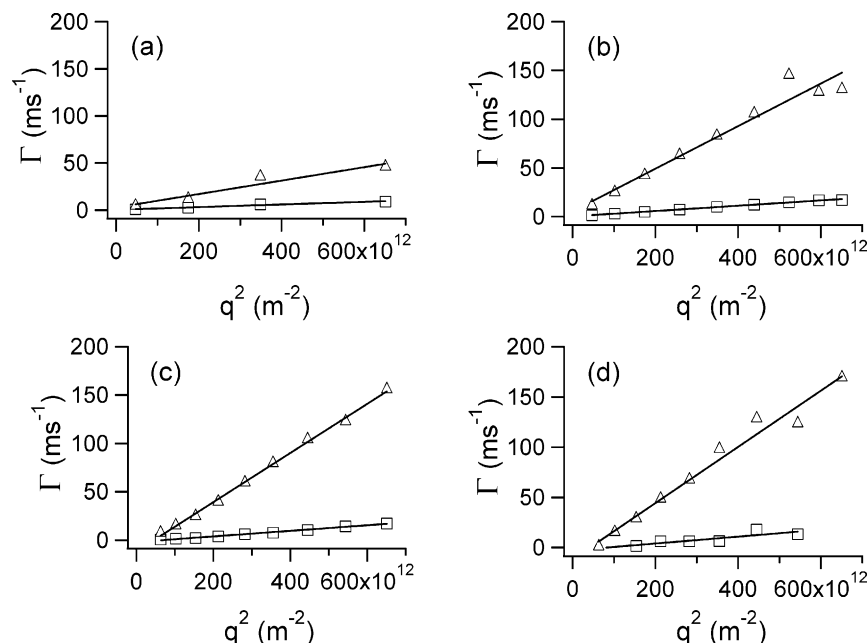


Figure 5. Fast (triangles) and slow (squares) relaxation rates against the squared wave vector for clear solutions with molar ratio TEOS/TPAOH/H₂O of 25:*x*:400 with (a) *x* = 5, (b) *x* = 9, (c) *x* = 13, and (d) *x* = 19.

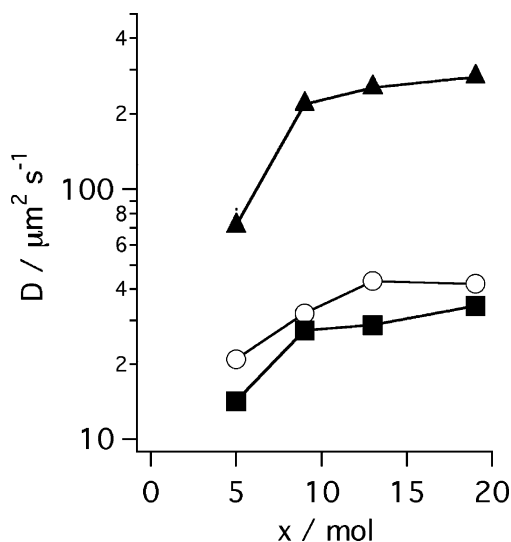


Figure 6. Diffusion coefficients D_f (triangles) and D_s (squares) determined from DLS and D_0 values estimated from SAXS–NMR (circles) for clear solutions with molar composition TEOS/TPAOH/H₂O of 25:*x*:400. Because error bars were smaller than figure captions they were omitted for clarity.

stems from the relaxation of large scale fluctuations of the local number density of the colloids. It is a fast process, also present in systems of monodisperse particles, and mainly depends on the strength of the interactions and the particle size.¹⁴ The slower diffusion mode is related to the self-diffusion in a population of particles which slightly differ in size and shape^{13b,14} or are polydisperse in particle charge.^{13a}

However, the current study of these nanoparticles in the different clear solutions does not allow deciding which type of polydispersity is at stake. Small deviations from one mean size and deviations from a spherical particle shape were observed using in situ atomic force microscopy (AFM) in dilute systems¹⁵ and are, therefore, likely to occur in the present more concentrated clear solutions as well.

Combining the observations of the NMR and DLS suggests that charge polydispersity also is present and could play a role in the aggregation of Silicalite-1 precursors. The colloidal interactions between the nanoparticles have important electrostatic repulsive components, notwithstanding the high ionic strengths.^{2a,10} Particle charge is expected to vary with the Q^n connectivity of the individual particles. The distribution of Q^n displays a dependence on clear solution composition (Figure 2b). Particles rich in Q^4 will have a lower electronic charge, because of their lower content of silanol groups per surface area that can be dissociated in the basic medium. The electrostatic repulsion between such particles is then reduced, leading to an enhanced probability for aggregation. Previous kinetic studies on heated clear solutions with molar TEOS/TPAOH/H₂O content of 25:*x*:480 with *x* varying from 3 to 11 have shown that the crystal growth decelerates in the range from *x* = 7 to *x* = 11.⁸

Previous in situ studies using AFM, X-ray scattering (XRS), transmission electron microscopy (TEM), and solid-state NMR on extracted particles suggested that particles in clear solutions already have an average structure resembling the final zeolite framework¹⁶ with fully condensed Q^4 Si atoms. In clear solutions with medium TPAOH content (*x* = 5 or 9), the small particles approaching best the zeolite connectivity are expected to be relatively little charged, increasing their probability to be united. The resulting self-assembled aggregates can be expected to be enriched in zeolite-like particles and may therefore act as crystal nuclei.

(15) Davis, T. M.; Drews, T. O.; Ramanan, H.; He, C.; Dong, J.; Schnablegger, H.; Katsoulakis, M. A.; Kokkoli, E.; McCormick, A. V.; Penn, L. R.; Tsapatsis, M. *Nat. Mater.* **2006**, *5*, 400.

(16) (a) Burkett, S. L.; Davis, M. E. *Chem. Mater.* **1995**, *7*, 920. (b) Magusin, P. C. M. M.; Zorin, V. E.; Aerts, A.; Houssin, C. J. Y.; Yakovlev, A. L.; Kirschhock, C. E. A.; Martens, J. A.; van Santen, R. A. *J. Phys. Chem. B* **2005**, *109*, 22767.

(14) Pusey, P. N.; Fijnaut, H. M.; Vrij, A. *J. Chem. Phys.* **1982**, *77*, 4270.

Conclusions

The properties of concentrated clear solutions with different TPAOH contents were investigated at room temperature with ^{29}Si NMR, SAXS, and DLS. Quantitative ^{29}Si NMR revealed the nature of the silicate species. Oligomeric species and particles were identified on the basis of line width, and the corresponding populations were quantified. The distribution over the populations and the connectivity of the particles were found to be strongly dependent on the molar TPAOH content. In systems commonly used for colloidal Silicalite-1 synthesis (TEOS/TPAOH/ H_2O of 25:5:400 and 25:9:400), the large majority of Si atoms has been shown to be contained in particles. Quantitative ^{29}Si NMR enables a clear interpretation of the SAXS data in terms of particle size. In clear solutions with a TEOS/TPAOH/ H_2O molar ratio of 25:19:400, the particles are very small and are interpreted as oligomer aggregates on the basis of the resemblance of their silicate connectivity. The colloid dynamics of the clear solution were monitored with DLS. The ACFs displayed two distinct diffusive modes. On the basis of particle sizes from the SAXS–NMR combination,

a physical interpretation of the two modes was possible. The faster process is the collective particle diffusion. The slow mode is due to self-diffusion and is detectable due to charge and/or size polydispersity of the particles. It can be used to estimate the equivalent hydrodynamic particle size. The role of the effect of particle size, shape, and charge polydispersity should be considered when modeling the zeolite assembly process.

Acknowledgment. The authors acknowledge F.W.O.-Vlaanderen and Prof. L. Wyns for their continuous support of the DUBBLE project. Nicolas Vilayphiou (DUBBLE, ESRF, Grenoble) is acknowledged for assistance during the synchrotron X-ray measurements. L.R.A.F., J.V., C.E.A.K., and J.A.M. acknowledge financial support by ESA and the Belgian Prodex office. A.A. and J.A.M. acknowledge the Flemish IWT for financial support via the SBO programme BIPOM. T.P.C. acknowledges the Flemish IWT for a Ph.D. scholarship. J.V. and B.L. acknowledge support of the NoE SoftComp (EU, 6Fp). B.G. is a postdoctoral fellow of FWO-Vlaanderen.

CM070693J